

Light-Switchable Exchange-Coupled Magnet

Divya Rajan,[†] John M. Cain,[†] Tatiana Brinzari,[§] Caue F. Ferreira,[†] Nicholas G. Rudawski,[‡] Ashley C. Felts,[†] Mark W. Meisel,^{*,§} and Daniel R. Talham^{*,†}

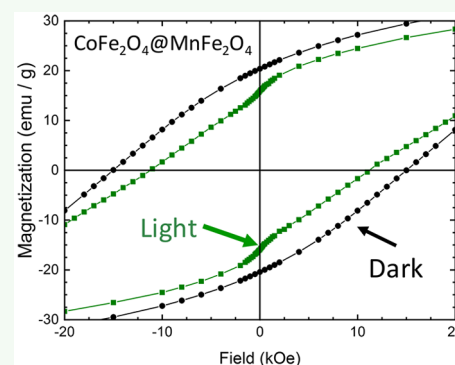
[†]Department of Chemistry, University of Florida, Gainesville, Florida 32611-7200, United States

[§]Department of Physics and National High Magnetic Field Laboratory, University of Florida, Gainesville, Florida 32611-8440, United States

[‡]Herbert Wertheim College of Engineering, University of Florida, Gainesville, Florida 32611, United States

Supporting Information

ABSTRACT: A light-switchable hard magnet/soft magnet composite is described for which light irradiation breaks the exchange coupling between the two components. Heterostructure composites composed of nanometer scale particles of the hard magnet cobalt ferrite with the soft magnet manganese ferrite show a coherent response in magnetization versus applied field measurements, consistent with exchange coupling, which is disrupted upon illumination, causing an inflection at low fields corresponding to the soft magnet manganese ferrite. The light-induced decoupling of the exchange-coupled magnets can be attributed to the selective demagnetization at the surface of the ferrite nanoparticles, breaking the interferrite coupling.



KEYWORDS: ferrite magnets, exchange coupling, cobalt ferrite, manganese ferrite, nanomagnets, light-induced magnetization

Larger magnetic data storage densities require smaller bit sizes, but even as smaller objects are realized, areal densities become limited by the ability to focus the magnetic write head. To overcome the limitations of write-head focusing, heat-assisted magnetic recording (HAMR)^{1–3} was developed, whereby a laser is used to locally heat the recording media and lower its energy product to enable recording on strongly anisotropic media. Manipulation of magnetization solely with light, or all-optical switching (AOS), has also been demonstrated for a growing list of potential recording media.⁴ In AOS, femtosecond laser pulses heat the magnetic system to near the Curie temperature, leading to magnetization switching dictated either by the choice of circular polarization or by magnetic sublattice structure.⁴ With these methods, magnetic information size becomes determined by standards of technologies such as plasmonic focusing or near-field optics, rather than by the ability to focus a magnetic field. However, a potential limitation of these technologies is thermal heating and cycling, which can cause component degradation.²

These drawbacks could be overcome if the energy product of a magnet can be lowered without the need for bulk heating. In this work, a light-switchable hard/soft exchange-coupled magnet is described, demonstrating a new concept with potential application in energy-assisted magnetic recording or switchable microwave absorption. Exchange-coupled magnets are nanocomposites with potential applications in diverse fields spanning from energy to biomedicine.^{5–9} Exchange coupling between a ferromagnet and antiferromagnet generates an extra source of anisotropy due to the component interface and a

consequent increase in the thermal stability of the magnetization.^{10,11} In another variation, when a hard permanent magnet is exchange coupled with a soft magnet having higher magnetization, the energy product of the composite is enhanced. The soft phase becomes enslaved to the hard phase, and the composite responds coherently to temperature and applied magnetic field.^{6,12,7,13} Studies have shown exchange-coupled magnets represent an effective approach to tackling the competing technical demands associated with miniaturizing magnets while at the same time maintaining viable properties, such as thermal stability of magnetization and coercivity, both of which decrease as magnetic particles approach the superparamagnetic limit.^{3,8,10}

The concept for a light-switchable exchange-coupled magnet derives from the fact that exchange coupling depends on interactions between moments at the interface between the two coupled materials.⁶ If exchange at the interface is broken, the soft component reverts, and the energy product of a hard magnet/soft magnet composite decreases. Therefore, a light-based process to selectively alter the interface coupling would eliminate the need for thermal heating of the bulk material. The recent observation of light-induced demagnetization in some cobalt ferrite and manganese ferrite nanoparticles provides an opportunity to demonstrate the concept. Cobalt

Received: August 14, 2019

Accepted: November 18, 2019

Published: November 18, 2019

ferrite nanoparticles were shown by Giri et al.^{14,15} to undergo a light-activated decrease in coercivity. A more recent study revealed white light irradiation also decreases high-field magnetization.¹⁶ The light-induced demagnetization effects were attributed to decoupling of the surface spins, leading to a change in volume of the magnetically ordered domains. The broken symmetry and reduced numbers of exchange pathways mean the surface spins decouple on a different energy scale than the bulk.^{17–22} A key observation was larger effects are seen for aggregates of particles relative to isolated nanoparticles, indicating the light process also reduces interparticle coupling.¹⁶ If the same processes are applied to a composite material pairing a hard magnet with a soft magnet, a light-switchable exchange-coupled magnet should result, providing a mechanism to amplify the effect of the light.

Examples of cobalt-ferrite-based exchange-coupled magnets are known with core–shell heterostructures, for example, FePt@CoFe₂O₄,²³ ZnFe₂O₄@CoFe₂O₄²⁴ and MnFe₂O₄@CoFe₂O₄.⁸ In this study, manganese ferrite was chosen as the soft magnet to couple with cobalt ferrite, building on our earlier work.¹⁶ Good epitaxy is expected, as the two ferrite materials have a relatively small lattice mismatch of around 1.7%.²⁵ Using surfactant-free coprecipitation methods, cobalt ferrite, **1**, and two cobalt ferrite/manganese ferrite particle composites, **2** and **3**, were prepared, as described in detail in the Supporting Information. The cobalt ferrite (Figure 1), with

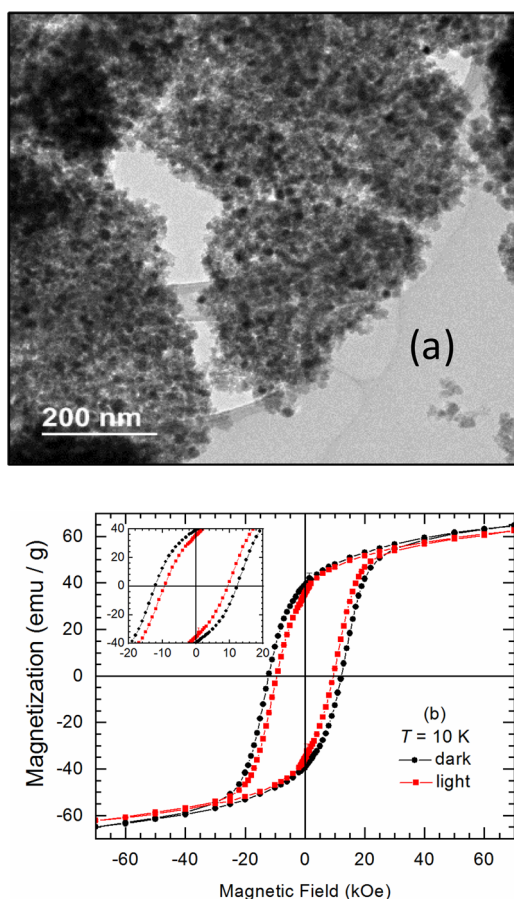


Figure 1. (a) TEM micrographs of Co_{0.94}Fe_{2.06}O₄, **1**. The particle size distribution within larger aggregates is 12 ± 4 nm (see Supporting Information for histogram). (b) Magnetization vs field hysteresis for **1** in the dark and light states at 10 K with an expanded view as an inset.

an average size of 12 ± 4 nm within aggregates of an average size of 250 ± 70 nm, was analyzed for Co_{0.94}Fe_{2.06}O₄ by ICP. These cobalt ferrite particles were used as seeds to generate a core–shell-like heterostructure of cobalt ferrite@manganese ferrite, **2**, following addition of the shell material precursors to a suspension of the seed particles. The resulting aggregates (Figure 2) have a size of 270 ± 80 nm and are composed of nanoparticles with an average size of 16 ± 4 nm. The ICP-AES analyses indicate the two ferrites are present in a 1:1 ratio, consistent with precursor amounts used in the synthesis. The small difference in the electron density of the two materials means there is no contrast between the two components in TEM micrographs, although energy dispersive X-ray spectroscopy line scans (Figure 2) reveal the elements Co, Mn, and Fe are uniformly detected across the particle aggregates, indicating the Mn_{0.94}Fe_{2.06}O₄ precipitates over the preformed Co_{0.94}Fe_{2.06}O₄ seeds. In contrast to **2**, which may be thought of as a core–shell-like heterostructure, **3** is a more intimate mixture, prepared by simultaneous precipitation of the two ferrites. For **3**, the aggregates average 250 ± 70 nm and the nanoparticles within the aggregates are somewhat smaller, with an average diameter of 4 ± 1 nm, Figure 3. The 2:1 cobalt:manganese ratio used in the synthesis is reflected in the 2:1 cobalt ferrite:manganese ferrite ratio determined by ICP-AES analyses of the products. Although the separate ferrites cannot be discerned in the electron microscopy, and some degree of ion mixing cannot be ruled out, observation of the two components in magnetic measurements and fitting of the powder XRD pattern (Supporting Information) confirm **3** is best described as a heterostructure composite rather than a solid solution.

Magnetization vs field plots for **1** at 10 K are shown in Figure 1 with and without white light irradiation. The dark-state coercivity of 12.17 ± 0.04 kOe decreases to 9.43 ± 0.09 kOe with light and is accompanied by a reduction in the remnant and high-field-magnetization values. This behavior with light is consistent with earlier reports^{14–16} on cobalt ferrite nanoparticles and has been attributed to decoupling of surface spins on the nanoparticles resulting in a reduction of magnetic volume and changing interparticle interactions within the aggregates.¹⁶ Similar magnetization vs field plots with and without light for the core–shell-like **2** are presented in Figure 2. The hysteresis loop in the absence of light indicates a coherent response of the two components to the applied magnetic field, consistent with an exchange-coupled system. The lack of contrast between the core and shell material in the TEM analyses does not clearly discern the shell component; however, the magnetization vs field response provides an upper limit to the thickness of the manganese ferrite shell. For an exchange-coupled system to coherently respond to temperature and field, the thickness of the soft phase should be less than twice the domain wall width of the hard magnet.^{23,26,13} The domain wall width of cobalt ferrite has been calculated to be 8 nm, indicating the manganese ferrite should be no thicker than 16 nm to give a coherent response.⁸ The change in particle size upon precipitating the manganese ferrite is less than 16 nm, which is within the expected requirements for an exchange-coupled heterostructure. Just as for cobalt ferrite, the coercivity of **2** decreases with light. The dark-state coercivity of 10.50 ± 0.01 kOe decreases to 8.28 ± 0.08 kOe, with a change of $\Delta H_c = 2.74 \pm 0.10$ kOe, which is comparable with the change seen for **1**. However, in contrast to **1**, there is a small inflection in the light-state plot for **2** near 1 kOe. Although the

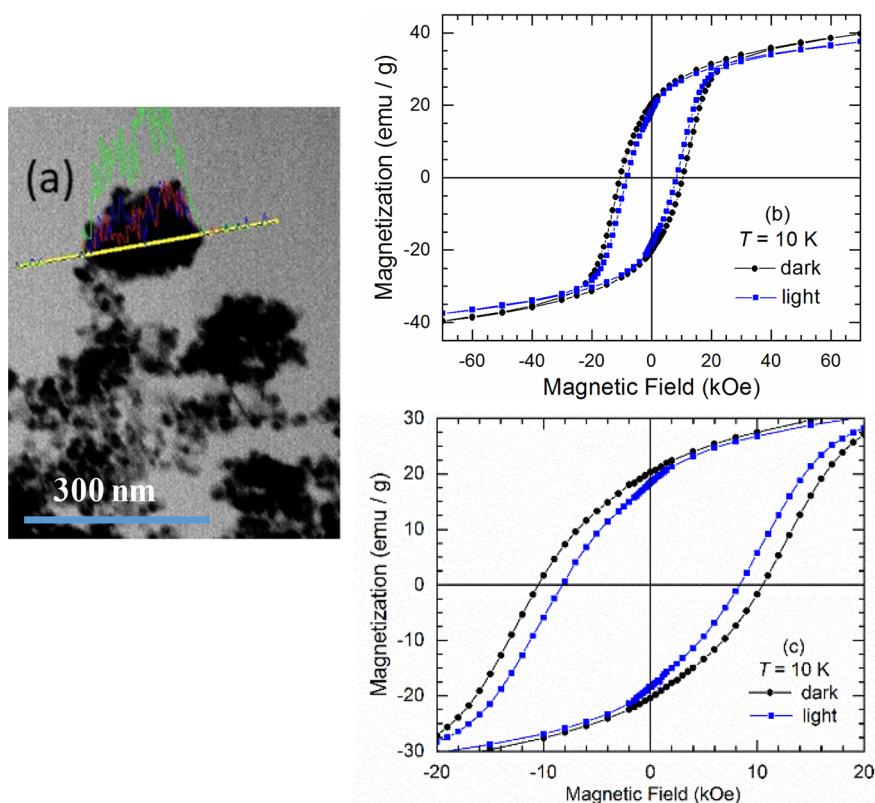


Figure 2. TEM image and magnetometry data for **2**. (a) TEM micrograph showing the aggregate on which the electron beam was scanned to obtain corresponding EDS line scans (particle size histogram and complete EDS scans appear in Supporting Information, Figure S2). (b) Magnetization vs field hysteresis for **2** in the dark and light states at 10 K swept ± 70 kOe. (c) Expanded view of the ± 20 kOe region from (b).

magnitude of the change is small, this low-field feature in the hysteresis loop indicates magnetic decoupling.

Exchange coupling in nanocomposite heterostructures depends critically on component dimensions and interface coupling,²⁷ and one-pot syntheses to increase contact between components have often resulted in better magnetic response.^{28–30} This approach was used for the synthesis of **3**, in which the hard and soft ferrites were coprecipitated, forming an intimate mixture of the two compounds. While magnetometry and PXRD confirm two components, TEM, EDS, and EELS analyses could not discern the separate ferrites, so individual compositional domains are no larger than a few nm. As for **2**, magnetization vs field plots for **3** show a coherent magnetic response with a coercivity of 15.01 ± 0.01 kOe at 10 K, Figure 3, again indicating an exchange-coupled mixture of cobalt ferrite–manganese ferrite. While the value of the coercive field for **2** was smaller than for the pure cobalt ferrite, **1**, the coercive field for **3** is larger. The behavior parallels observations by Song et al.⁸ for exchanged-coupled $\text{CoFe}_2\text{O}_4@ \text{MnFe}_2\text{O}_4$ nanoparticles prepared by thermal decomposition techniques, where the coercive field first increased upon addition of a thin, ~ 1 nm, manganese ferrite shell but then decreased for successively thicker shells. Once again, upon irradiation with white light, the coercivity decreases, Figure 3. For **3**, the change, $\Delta H_c = 3.80 \pm 0.01$ kOe, is even larger than seen for the pure-phase cobalt ferrite. However, the most striking feature is a significant inflection in the light state at low field resulting from magnetic decoupling of the cobalt ferrite and manganese ferrite with light.

Magnetization vs field of **3** was measured at different temperatures in the dark to confirm the presence of exchange-

coupled ferrites and explore the thermal requirements needed to break the exchange coupling. At 10 K, the system is exchange-coupled, but with increasing temperature, an inflection appears at low field, corresponding to the soft magnet, Figure 4. The system is effectively decoupled by 50 K, which is expected to be above the blocking temperature of manganese ferrite nanoparticles.⁸ Based on work on other materials using the same light source and temperature control, we estimate the temperature change of the sample caused by the light source is ≤ 0.5 K for temperatures below 50 K. Nevertheless, to verify the observed light-activated changes in the coercivity, remnant and high-field magnetization, and magnetization at 70 kOe of **3** were compared to the dark-state values at different temperatures in Figure 4. The light-state values of the coercivity and remnant magnetization at 10 K were comparable to their respective dark-state values at ~ 25 –30 K, corresponding to a temperature jump well outside experimental control. Furthermore, high-field magnetization in the light state at 10 K is significantly smaller than the high-field value, even at 50 K, providing further evidence the light-state response is not a result of bulk heating.

The light-induced decoupling of the exchange-coupled magnets can be attributed to the selective demagnetization of the surface spins of the ferrite nanoparticles, as was recently described for single-phase cobalt ferrite and manganese ferrite.¹⁶ For the single-phase ferrites, the light-induced decreases in magnetic coercivity and high-field magnetization can be attributed to changes in magnetic volume, as irradiation decouples the weakly coupled surface spins of the high surface-to-volume ratio nanoparticles.¹⁶ The likely explanation for the

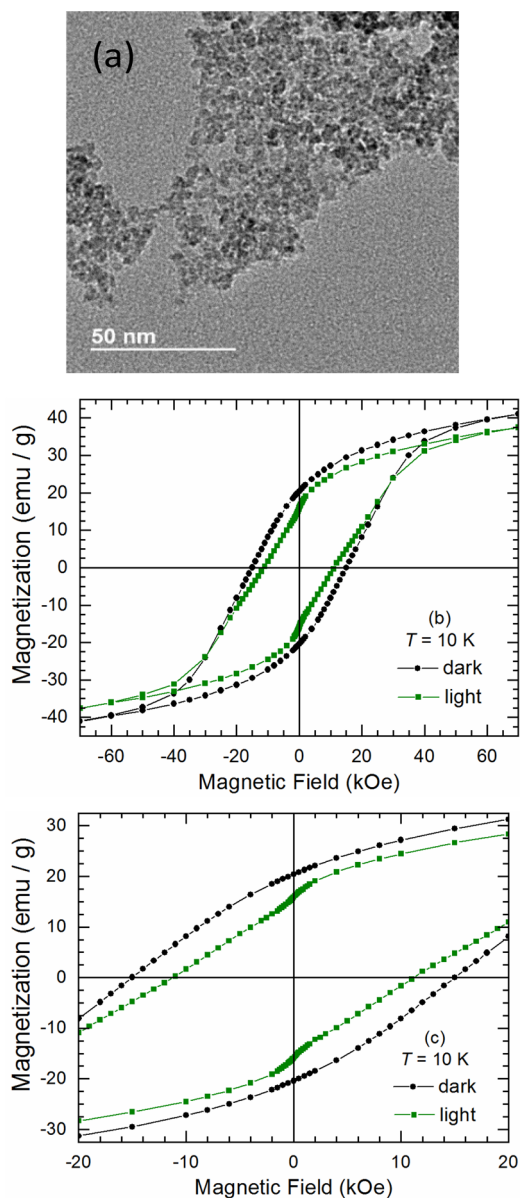


Figure 3. TEM image and magnetometry data for 3. (a) TEM micrograph (particle size histogram and EELS analysis appear in Supporting Information, Figure S3). (b) Magnetization vs field hysteresis for 3 in the dark and light states at 10 K swept ± 70 kOe. (c) Expanded view of the ± 20 kOe region of (b).

surface selectivity is effective heating of the electronic reservoir near the surface mediated by skin-depth absorption. At low temperatures, the electronic reservoir can be effectively decoupled from the macroscopic lattice, limiting the light-induced thermal jump to the surface spins, which experience weaker magnetic coupling than the bulk because of surface disorder and lower number of nearest neighbors. For the previously studied cobalt ferrite, the light-induced effects were larger for aggregates than for nanoparticles isolated by surfactant coatings, as the surface spin decoupling also weakened interparticle coupling. In exchange-coupled heterostructures, selective demagnetization of the surface spins is sufficient to break the exchange coupling while maintaining the bulk magnetization of the two constituents, as observed for compositions 2 and 3.

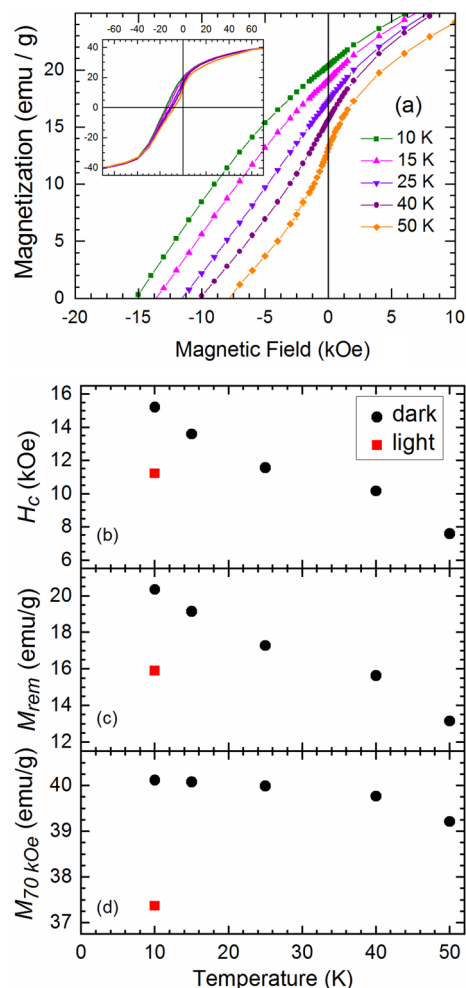


Figure 4. (a) Magnetization vs field hysteresis for 3 in the dark at different temperatures. (b–d) Comparisons of the light-activated changes of coercivity, remnant magnetization, and magnetization at 70 kOe for 3 at 10 K to the dark-state values of the same sample over the temperature range of 10–50 K.

The present study takes advantage of the concept of using light-induced changes in surface magnetization to design an exchange-coupled magnet that can be switched with light. At the same time, the results on the cobalt ferrite/manganese ferrite heterostructures validate the recently proposed explanation for the light-induced demagnetization in ferrite nanoparticles, upon which the current study was based.¹⁶ The results provide a new mechanism for designing light-switchable magnetic materials. Using light to decouple exchange-coupled magnets is a potential route to decreasing the energy product of a magnetic bit and enabling magnetic recording at lower write-head magnetic fields. Since it is only necessary to influence the surface spins, bulk laser heating of the magnetic medium is not required, which could have a great impact on potential applications.

■ ASSOCIATED CONTENT

Supporting Information

The Supporting Information is available free of charge at <https://pubs.acs.org/doi/10.1021/acsaelm.9b00520>.

Synthesis and methods, chemical and particle size analysis, PXRD refinement for 3 (PDF)

AUTHOR INFORMATION

Corresponding Authors

*E-mail: talham@chem.ufl.edu. (D.R.T.)

*E-mail: meisel@phys.ufl.edu. (M.W.M.)

ORCID

Daniel R. Talham: 0000-0003-1783-5285

Notes

The authors declare no competing financial interest.

ACKNOWLEDGMENTS

This work was supported in part by the following funding sources: The National Science Foundation via DMR-1405430 and DMR-1904596 (D.R.T.), DMR-1202033 and DMR-1708410 (MWM), and DMR-1157490 and DMR-1644779 (National High Magnetic Field Laboratory) and the University of Florida Division of Sponsored Programs. Use of the Advanced Photon Source at Argonne National Laboratory was supported by the U.S. Department of Energy, Office of Science, Office of Basic Energy Sciences, under Contract No. DE-AC02-06CH11357.

REFERENCES

- (1) Challener, W.; Peng, C.; Itagi, A.; Karns, D.; Peng, W.; Peng, Y.; Yang, X.; Zhu, X.; Gokemeijer, N.; Hsia, Y.; Ju, G.; Rottmayer, R.; Seigler, M.; Gage, E. Heat-assisted magnetic recording by a near-field transducer with efficient optical energy transfer. *Nat. Photonics* **2009**, *3*, 220–224.
- (2) McDaniel, T. Areal density limitation in bit-patterned, heat-assisted magnetic recording using FePtX media. *J. Appl. Phys.* **2012**, *112*, 093920.
- (3) Elphick, K.; Vallejo-Fernandez, G.; Klemmer, T.; Thiele, J.; O'Grady, K. HAMR media based on exchange bias. *Appl. Phys. Lett.* **2016**, *109*, 052402.
- (4) El Hadri, M.; Hehn, M.; Malinowski, G.; Mangin, S. Materials and devices for all-optical helicity-dependent switching. *J. Phys. D: Appl. Phys.* **2017**, *50*, 133002.
- (5) Liu, F.; Hou, Y.; Gao, S. Exchange-coupled nanocomposites: chemical synthesis, characterization and applications. *Chem. Soc. Rev.* **2014**, *43*, 8098–8113.
- (6) Bader, S. D. Opportunities in nanomagnetism. *Rev. Mod. Phys.* **2006**, *78*, 1–15.
- (7) López-Ortega, A.; Estrader, M.; Salazar-Alvarez, G.; Roca, A. G.; Nogués, J. Applications of exchange coupled bi-magnetic hard/soft and soft/hard magnetic core/shell nanoparticles. *Phys. Rep.* **2015**, *553*, 1–32.
- (8) Song, Q.; Zhang, Z. J. Controlled Synthesis and Magnetic Properties of Bimagnetic Spinel Ferrite CoFe_2O_4 and MnFe_2O_4 Nanocrystals with Core-Shell Architecture. *J. Am. Chem. Soc.* **2012**, *134*, 10182–10190.
- (9) Rostamnejadi, A.; Venkatesan, M.; Salamati, H.; Ackland, K.; Gholizadeh, H.; Kameli, P.; Coey, J. Magnetic properties, exchange bias, and memory effects in core-shell superparamagnetic nanoparticles of $\text{La}_{0.67}\text{Sr}_{0.33}\text{MnO}_3$. *J. Appl. Phys.* **2017**, *121*, 173902.
- (10) Skumryev, V.; Stoyanov, S.; Zhang, Y.; Hadjipanayis, G.; Givord, D.; Nogués, J. Beating the superparamagnetic limit with exchange bias. *Nature* **2003**, *423* (6942), 850.
- (11) Phan, M.-H.; Alonso, J.; Khurshid, H.; Lampen-Kelley, P.; Chandra, S.; Stojak Repa, K.; Nemati, Z.; Das, R.; Iglesias, O.; Srikanth, H. Exchange Bias Effects in Iron Oxide-Based Nanoparticle Systems. *Nanomaterials* **2016**, *6*, 221.
- (12) Liu, J.P. Exchange-Coupled Nanocomposite Permanent Magnets. *Nanoscale Magnetic Materials and Applications* **2009**, 309.
- (13) Nandwana, V.; Chaubey, G. S.; Yano, K.; Rong, C.-B.; Liu, J. P. Bimagnetic nanoparticles with enhanced exchange coupling and energy products. *J. Appl. Phys.* **2009**, *105* (1), 014303.
- (14) Giri, A. K.; Pellerin, K.; Pongsaksawad, W.; Sorescu, M.; Majetich, S. A. Effect of light on the magnetic properties of cobalt ferrite nanoparticles. *IEEE Trans. Magn.* **2000**, *36*, 3029–3031.
- (15) Giri, A. K.; Kirkpatrick, E. M.; Moongkhamklang, P.; Majetich, S. A.; Harris, V. G. Photomagnetism and structure in cobalt ferrite nanoparticles. *Appl. Phys. Lett.* **2002**, *80*, 2341–2343.
- (16) Brinzari, T.; Rajan, D.; Ferreira, C.; Stoian, S.; Quintero, P.; Meisel, M.; Talham, D. Light-induced magnetization changes in aggregated and isolated cobalt ferrite nanoparticles. *J. Appl. Phys.* **2018**, *124*, 103904.
- (17) Haneda, K.; Morrish, A. H. Noncollinear magnetic-structure of CoFe_2O_4 small particles. *J. Appl. Phys.* **1988**, *63*, 4258–4260.
- (18) Kodama, R. H.; Berkowitz, A. E.; McNiff, E. J., Jr; Foner, S. Surface spin disorder in NiFe_2O_4 nanoparticles. *Phys. Rev. Lett.* **1996**, *77*, 394–397.
- (19) Morales, M. P.; Veintemillas-Verdaguer, S.; Montero, M. I.; Serna, C. J.; Roig, A.; Casas, L.; Martinez, B.; Sandiumenge, F. Surface and internal spin canting in $\gamma\text{-Fe}_2\text{O}_3$ nanoparticles. *Chem. Mater.* **1999**, *11*, 3058–3064.
- (20) Krycka, K.; Borchers, J.; Booth, R.; Ijiri, Y.; Hasz, K.; Rhyne, J.; Majetich, S. Origin of Surface Canting within Fe_3O_4 Nanoparticles. *Phys. Rev. Lett.* **2014**, *113*, 147203.
- (21) Ijiri, Y.; Krycka, K.; Hunt-Isaak, I.; Pan, H.; Hsieh, J.; Borchers, J.; Rhyne, J.; Oberdick, S.; Abdelgawad, A.; Majetich, S. Correlated spin canting in ordered core-shell $\text{Fe}_3\text{O}_4/\text{Mn}_x\text{Fe}_{3-x}\text{O}_4$ nanoparticle assemblies. *Phys. Rev. B: Condens. Matter Mater. Phys.* **2019**, *99*, 094421.
- (22) Oberdick, S.; Abdelgawad, A.; Moya, C.; Mesbahi-Vasey, S.; Kepaptsoglou, D.; Lazarov, V.; Evans, R.; Meilak, D.; Skoropata, E.; van Lierop, J.; Hunt-Isaak, I.; Pan, H.; Ijiri, Y.; Krycka, K.; Borchers, J.; Majetich, S. Spin canting across core/shell $\text{Fe}_3\text{O}_4/\text{Mn}_x\text{Fe}_{3-x}\text{O}_4$ nanoparticles. *Sci. Rep.* **2018**, *8*, 3425.
- (23) Zeng, H.; Sun, S.; Li, J.; Wang, Z. L.; Liu, J. P. Tailoring magnetic properties of core/shell nanoparticles. *Appl. Phys. Lett.* **2004**, *85*, 792–794.
- (24) Masala, O.; Hoffman, D.; Sundaram, N.; Page, K.; Proffen, T.; Lawes, G.; Seshadri, R. Preparation of magnetic spinel ferrite core/shell nanoparticles: Soft ferrites on hard ferrites and vice versa. *Solid State Sci.* **2006**, *8*, 1015–1022.
- (25) Brabers, V.A.M. Progress in spinel ferrite research. *Handbook of Magnetic Materials* **1995**, *8*, 189–324.
- (26) Skomski, R.; Coey, J. M. D. Giant energy product in nanostructured two-phase magnets. *Phys. Rev. B: Condens. Matter Mater. Phys.* **1993**, *48*, 15812.
- (27) Xie, Y.; Vincent, A.; Chang, H.; Rinehart, J. Strengthening nanocomposite magnetism through microemulsion synthesis. *Nano Res.* **2018**, *11*, 4133–4141.
- (28) Pahwa, C.; Mahadevan, S.; Narang, S.; Sharma, P. Structural, magnetic and microwave properties of exchange coupled and non-exchange coupled $\text{BaFe}_{12}\text{O}_{19}/\text{NiFe}_2\text{O}_4$ nanocomposites. *J. Alloys Compd.* **2017**, *725*, 1175.
- (29) Almessiere, M.; Slimani, Y.; Baykal, A. Exchange spring magnetic behavior of $\text{Sr}_{0.3}\text{Ba}_{0.4}\text{Pb}_{0.3}\text{Fe}_{12}\text{O}_{19}/(\text{CuFe}_2\text{O}_4)_x$ nanocomposites fabricated by a one-pot citrate sol-gel combustion method. *J. Alloys Compd.* **2018**, *762*, 389–397.
- (30) Hazra, S.; Patra, M.; Vadera, S.; Ghosh, N. A Novel But Simple “One-Pot” Synthetic Route for Preparation of $(\text{NiFe}_2\text{O}_4)_x(\text{BaFe}_{12}\text{O}_{19})_{1-x}$ Composites. *J. Am. Ceram. Soc.* **2012**, *95*, 60–63.